Isotopic composition of daily precipitation along southern foothills of the Himalayas: impact of marine and continental sources of atmospheric moisture

Ghulam Jeelani[1], Rajendrakumar D. Deshpande[2], Michal Galkowski[3], Kazimierz Rozanski[3]

[1]Department of Earth Sciences, University of Kashmir, Srinagar 190006, India
[2]Geosciences Division, Physical Research Laboratory (PRL), Navrangpura, Ahmedabad 380009, India
[3]Faculty of Physics and Applied Computer Science, AGH University of Science and Technology, Krakow 30-059, Poland

Correspondence to: Ghulam Jeelani (geojeelani@gmail.com)

Ghulam Jeelani

Department of Earth Sciences, University of Kashmir, Srinagar 190006, India

Email: geojeelani@gmail.com

Rajendrakumar D. Deshpande

[2]Geosciences Division, Physical Research Laboratory (PRL), Navrangpura, Ahmedabad 380009, India
Email: desh@prl.res.in

Michal Galkowski

Faculty of Physics and Applied Computer Science, AGH University of Science and Technology, Krakow 30-059, Poland

Email.: michal.galkowski@fis.agh.edu.pl

Kazimierz Rozanski

Faculty of Physics and Applied Computer Science, AGH University of Science and Technology, Krakow 30-059, Poland

Email.: rozanski@agh.edu.pl

Abstract. The flow of the Himalayan rivers, a key source of fresh water to more than a billion people primarily depends upon the strength, behaviour and duration of Indian Summer Monsoon (ISM) and Western Disturbances (WD), two contrasting circulation regimes of the regional atmosphere. Analysis of ^{2}H and ^{18}O isotope composition of daily precipitation collected along the southern foothills of the Himalayas, combined with extensive backward trajectory modelling, was used to gain deeper insight into the mechanisms controlling isotopic composition of precipitation and the origin of atmospheric moisture and precipitation during ISM and WD periods. Daily precipitation samples have been collected during the period September 2008 - December 2011 at six stations, extending from Srinagar in the west (Kashmir state) to Dibrugarh in the east (Assam state). In total, 548 daily precipitation samples have been collected and analysed for their stable isotope composition. It is suggested that gradual reduction in ^{2}H and ^{18}O content of precipitation in the studied region, progressing from $\delta^{18}O$ values close to zero down to ca. -10 ‰ in the course of ISM evolution, stems from regional, large-scale recycling of moisture-driven monsoonal circulation. Superimposed on this general trend are short-term fluctuations of the isotopic composition of rainfall, which might have their roots in the local effects such as enhanced convective activity and associated higher degree of rainout of moist air masses (local amount effect), partial evaporation of raindrops or impact of isotopically heavy moisture generated in evapotranspiration processes taking place in the vicinity of rainfall sampling sites. Seasonal footprint maps constructed for three stations representing western, central and eastern portion of the Himalayan region indicate that influence of monsoonal circulation reaches western edges of the Himalayan region. While characteristic imprint of monsoon air masses (increase of monthly rainfall amount) can be completely absent in the western Himalaya, the onset of ISM period in this region is still clearly visible in the isotopic composition of daily precipitation. Characteristic feature of daily precipitation collected during WD period is a gradual increase of ^{2}H and ^{18}O content, reaching positive $\delta^{2}H$ and $\delta^{18}O$ values towards the end of this period. This trend can be explained by growing importance of moisture of continental origin as a source of daily precipitation. High d-excess values of daily rainfall recorded at the monitoring stations (38 cases in total, range from 20.6 to 44.0 ‰) are attributed to moisture of continental origin released into the atmosphere during evaporation of surface water bodies and/or soil water evaporation.

1 Introduction

The Himalayas are a 2900 km long, west-northwest to east-southeast trending mountain range, which began to form between 40 and 50 Ma ago due to the collision of two large landmasses, India and Eurasia. This immense mountain range shapes the climate of southeast Asia and the northern Hemisphere (e.g. Clemens et al., 1991; Molnar et al., 2010). The regional climate of the Himalayas is dominated by two distinct circulation regimes of the regional atmosphere: the Indian Summer Monsoon (ISM) and the Western Disturbances (WD) periods.

The ISM is one of the most energetic components of the earth's climate system, which develops in response to the movement of Inter Tropical Convergence Zone (ITCZ) that separates atmospheric circulation of the northern and southern hemispheres (e.g. Gadgil, 2003; Allen and Armstrong 2012). The warming of the Tibetan Plateau relative to the Indian Ocean, resulting in low pressure over Asia and higher pressure over the Indian Ocean (Overpeck et al*.,* 1996), pulls moisture from Southeast Asia and the Bay of Bengal and transports it north-westward (Hren, et al., 2009; Li et al., 2016). There is an east-west gradient in monsoonal influence across the Himalaya with the central Himalayas receiving according to some estimates up to 80% of its annual precipitation during the monsoon months (Bookhagen and Burbank, 2010; Lang and Barros, 2004).

Western Disturbances are eastward moving synoptic low-pressure systems embedded in the lower to mid-tropospheric westerlies in subtropics and originate from the Mediterranean Sea or mid-West Atlantic Ocean (Dimri et al., 2004; Dimri et al. 2015; Maharana and Dimri, 2014; Madhura et al., 2015, Rao and Srinivasan, 1969; Pisharoty and Desai, 1956). At times, secondary system of winds with embedded troughs develop over the Persian Gulf and the Black Sea either directly or as a result of the arrival of low-pressure systems from southwest Arabia (Dimri et al., 2004). Western Disturbances cause heavy precipitation (>50 % of annual precipitation in winter) in the western Himalayas (Lang and Barros, 2004) and northern India from December to April (Pisharoty and Desai, 1956; Mooley, 1957; Agnihotri and Singh, 1982). They are also found to be active during summer months as well, but with low frequency (Dhar et al., 1984; Dimri, 2006). When the troughs in the mid-tropospheric westerlies extent southwards into lower latitudes, the WD reach Afghanistan, Pakistan and India and get intensified by the moisture drawn from the Arabian Sea (Chand and Singh, 2015). Cannon et al., (2015) have shown that the heavy precipitation events occurring in western and central Himalayas due to WD are spatiotemporally independent. The strength and frequency of WD for the last three decades (1979-2010) has increased in western and decreased in central Himalayas. On the basis of the variation in the d-excess values of Ganga river water at Rishikesh, it was suggested that the snow-melt and ice-melt component has a significant fraction derived from winter precipitation with moisture source from mid-latitude westerlies (Maurya et al., 2011). The impact of climate change on the frequency and magnitude of precipitation events in the tropics is still a matter of debate (Held and Soden, 2006; Wentz et al., 2007; Allan and Soden, 2008). This may be partly due to inadequate understanding of the atmospheric water vapour dynamics (IPCC, 2013).

The flow of the Himalayan rivers, a key source of fresh water to more than a billion people (Ives and Messerli, 1989) primarily depends upon the strength, behaviour and duration of WD and ISM. The rivers support one of the most heavily irrigated regions in the world (Tiwari et al., 2009) and hydropower generation, the backbone of the region's economy (Karim and Veizer, 2002*;* Archer et al., 2010; Jeelani et al., 2012). Abnormal precipitation brought by WD and ISM can lead to flooding or drought, thereby affecting regional economies. It is therefore important to study spatiotemporal variability of ISM and WD in the Himalayas and to better characterize its causes and consequences. This implies, among others, better understanding of the sources of atmospheric moisture forming precipitation in the region during the two contrasting circulation regimes of the lower atmosphere.

The stable isotope composition of oxygen and hydrogen in water molecules is a powerful tool for studies of the hydrological cycle, both with respect to its present status as well as its past behaviour. In the modern environment, the isotopic composition of precipitation serves as a conservative tracer for the origin, phase transitions, and transport pathways of water (e.g. Dansgaard, 1964; Rozanski et al., 1993; Gat, 1996; Araguas-Araguas et al., 2000). The ^{18}O and ^{2}H content in precipitation are controlled by (i) atmospheric parameters such as temperature, degree of rainout of the moist air masses and the amount of rainfall (e.g. Dansgaard, 1964; Yurtsever and Gat, 1981; Rozanski et al., 1982; Rozanski et al., 1993), and (ii) by geographic factors such as altitude, latitude, moisture sources and atmospheric transport processes (e.g. Craig, 1961*;* Siegenthaler and Oeschger, 1980; Gat, 1996; Kendall and Coplen, 2001; Karim and Veizer, 2002). The $\delta^{2}H$ and $\delta^{18}O$ values in precipitation are tightly correlated and form a so-called Global Meteoric Water Line (GMWL) in the $\delta^{2}H$-$\delta^{18}O$ space, defined by the following relationship: $\delta^{2}H=8\cdot\delta^{18}O+10$ (Craig, 1963). A secondary isotope parameter, deuterium excess ($d = \delta^{2}H - 8\cdot\delta^{18}O$; Dansgaard, 1964) defines the position of data points in the $\delta^{2}H$-$\delta^{18}O$ space with respect to GMWL. The isotopic patterns of precipitation in the tropics are expected to be different from the sub-tropics and temperate regions due to large scale convection systems, cyclonic storms and multitude of vapour sources (e.g. Midhun et al., 2013; Lekshmy et al., 2014; Lekshmy et al., 2015). Consequently, the well-established isotope effects such as amount effect, temperature effect and altitude effect are not clearly visible in precipitation isotope data sets available for the Indian subcontinent (Deshpande and Jeelani 2017; Deshpande and Gupta, 2012; Deshpande et al., 2010; Warrier et al., 2010; Yavada et al., 2007). However, at local or watershed scale, stable water isotopes of precipitation showed a good relationship with altitude and temperature (Jeelani et al., 2017a, 2015, 2013; Kumar et al., 2010). The abrupt change in stable water isotopic values and the d-excess of precipitation during summer has been attributed to the reversal/change in the source of precipitation from western disturbances to south-west monsoons (Jeelani et al 2017b; Breitenbach et al., 2010).

The present study was launched with three major objectives: (i) to assess the seasonal variability of $\delta^{18}O$ and $\delta^{2}H$ in daily precipitation along the southern foothills of the Himalayas, (ii) to identify dominant moisture sources for precipitation in this region, and (iii) to demarcate the influence of Indian Summer Monsoon and Western Disturbances in the study area.

2 Study area

Daily precipitation samples were collected at six stations located along southern foothills of the Himalayas (Fig. 1 and Table 1). The stations cover the distance of almost 2900 km, from Srinagar in the west (Kashmir state) to Dibrugarh in the east (Assam state). In total, 548 daily precipitation samples have been collected and analysed. The largest number of samples was available for Jorhat (242) and Srinagar (121) stations. The stations are open to Indian subcontinent from the south and shielded by the Himalayan massif from the north. The elevation of the stations ranges from 99 m a.s.l. (Jorhat) to 1872 m a.s.l. (Ranichauri). The mean annual temperature varies from 13.6 ^{o}C (Srinagar) to 24.2 ^{o}C (Jammu) whereas the mean annual precipitation ranges from 693 mm at Srinagar to 2781 mm at Dibrugarh.

Fig.1 and Table 1 around here

Figure 2 shows long-term (1985-2014) monthly surface air temperature and precipitation data for six stations where daily precipitation samples have been collected. The data shown in Fig. 2 were grouped into two periods (Table 2): (i) Indian Summer Monsoon, and (ii) Western Disturbances period. The onset and duration of ISM was defined operationally on the basis of seasonal distribution of long-term monthly rainfall, and through examination of individual backward trajectories calculated for daily rainfall data gathered in the framework of the present study, available for each site (cf. section 4.1). The duration of ISM varies from 3 months (July-September) for the stations located at the western edge (Srinagar, Jammu, Palampur) to 5 months (May-September) for the stations located at the eastern edge of the transect (Jorthat, Dibrugarh). For the central part of the transect (stations Ranichauri and Kathmandu) the onset of ISM was set at the beginning of June and the termination at the end of September. Except for Srinagar station, the onset of ISM is marked by distinct increase of monthly rainfall amount (cf. Fig. 2). Although for Srinagar station the rainfall imprint of ISM onset and duration is not present, it could still be defined on the basis of backward trajectory analyses of the air masses associated with daily rainfall at this site, as well as through characteristic ^{18}O and ^{2}H isotope signatures of this rainfall.

Long-term mean values of surface air temperature and cumulative precipitation amount, calculated for ISM and WD periods, are reported in Table 2 for the stations where daily precipitation samples for isotope analyses were collected in the framework of this study. Also, the peak-to-peak amplitude of seasonal changes of monthly air temperature is reported. This amplitude increases gradually from the eastern (Dibrugarh: 11.7^{o}C) to the western edge of the transect (Srinagar: 23.1^{o}C), indicating progressive transition from maritime to continental climate. The mean temperatures for ISM and WD periods also differ, the former being significantly higher. The average difference is approximately 8^{o}C.

Fig.2 and Table 3 around here

The stations not only differ with respect to annual amount of rainfall (Table 1) but also with respect to cumulative rainfall amounts for ISM and WD periods, the former being generally higher (Table 2). The striking exception is Srinagar station - here the amount of rainfall during WD period is significantly higher (543 mm) than that during ISM period (150 mm). The ratio of cumulative rainfall amount during ISM and WD periods (parameter R in Table 2) varies from 3.41 for Dibrugarh to 1.95 for Ranichauri. For Srinagar, the value of this parameter is significantly lower than one (0.28).

3. Methods

Central Research Institute for Dryland Agriculture (CRIDA) and India Meteorological Department (IMD) collected most of the precipitation samples under the aegis of the National Program (IWIN) for isotope fingerprinting of waters of India (Deshpande and Gupta, 2008; Deshpande and Gupta, 2012). The Indian Meteorological Department, New Delhi, from its sub-offices, provided relevant meteorological data for the stations. Deuterium and ^{18}O isotope composition of rainfall samples was analysed using IWIN-IRMS facility at Physical Research Laboratory (PRL) Ahmadabad, following standard equilibration method in which water samples were equilibrated with CO_2 (or H_2) and the equilibrated CO_2 (or H_2) gas was analysed in Delta V Plus using isotope ratio mass spectrometry (IRMS) in continuous flow mode using Gasbench II (Maurya et al., 2009). The analytical uncertainty of isotope analyses (one sigma) was ±1.0‰ and ±0.1‰ for δ^2H and $\delta^{18}O$, respectively.

Reconstruction of backward trajectories of the air masses arriving at sampling stations was done through the framework of the Hybrid Single Particle Lagrangian Integrated Trajectory model (Hysplit4, revision February 2016 - Stein et al., 2015). The model was driven by archived Global Data Assimilation System (GDAS1 product, available at ftp://arlftp.arlhq.noaa.gov/pub/archives/gdas1) meteorological data available for every 3 h at 1.0°x1.0° horizontal resolution (corresponding to approx. 100 km x 100 km), with 23 sigma pressure layers between 1000 hPa and 20 hPa (Parrish and Derber, 1992). All trajectories were calculated with temporal resolution of 30 minutes. For each location, the trajectory release point has been set up at 500 m above the local ground level, in order to represent mean elevation of moist air masses.

Ten-day backward trajectories representing daily rainfall samples were calculated as trajectory ensembles, each consisting of twenty seven ensemble members released at 12:00 LT on the day with precipitation sample collection. Ensembles were produced by varying the initial trajectory wind speeds and pressures, according to the Hysplit ensemble algorithm, in order to account for the uncertainties involved in the simulation of individual backward trajectories. A slight modification of the default algorithm was used, with horizontal range of sampling of the initial values reduced from 1 to 0.5 width of the grid cell in the driving meteorological field. As no information about exact timing of precipitation events (except of the date) was available, the question of representativity of backward trajectories released at 12:00LT was investigated in some detail. For selected events multiple releases (every three hours) were realized for the given day. The results did not reveal any significant changes in ensemble patterns, neither in terms of trajectory source areas, nor in the behaviour of presented meteorological variables. Apparently, the ensemble scheme largely captures the variability of the transport patterns associated with generation of rainfall events sampled at the stations.

For footprint analysis, individual 10-day backward trajectories starting from 12:00 LT were calculated for each station collecting daily rainfall and for Kathmandu station, Nepal, representing central region of the transect. Daily releases over the course of three consecutive years (2009-2011) were simulated. The chosen period corresponds with the period of precipitation sampling at the stations. Daily trajectories calculated over the three-year period were then aggregated to produce the footprint maps. Footprints representative for ISM and WD seasons were calculated using the subsets of available trajectories. The output was a 0.5°x0.5° footprint signal, which was later smoothed spatially using focal averaging method.

4 Results and Discussion

4.1 Seasonality of isotope characteristics of daily rainfall

Figure 3 shows seasonal changes of $\delta^{18}O$ and deuterium excess for two stations with largest number of daily isotope data available (Jorhat - 242 data points, and Srinagar - 121 data points). These two stations are located on western (Srinagar) and eastern (Jorhat) edges of the studied transect (cf. Fig. 1). They have been selected to illustrate seasonal evolution of the isotopic composition of daily precipitation at the stations along the studied east-west transect. Figure S1 in the Supplement summarizes $\delta^{18}O$ and deuterium excess records available for other four stations. The ^{18}O isotope composition of daily precipitation at Jorhat and Srinagar stations shown in Fig. 3a reveals a distinct seasonality, particularly well seen in the data available for Jorhat station. During development of Indian Summer Monsoon, the ^{18}O content in daily precipitation at this site decreases gradually, from $\delta^{18}O$ values fluctuating around 0‰ at the onset of ISM, to very negative $\delta^{18}O$ values (up to ca. -20‰) recorded at its termination. During WD period the ^{18}O content progressively increases, reaching positive δ values towards the end of this period. The seasonality of ^{18}O signal is also well marked at other stations (Fig. S1a). As suggested by Fig. 3a, the largest heavy isotope depletion in rainfall is expected at the transition from ISM to WD period. Indeed, three most negative $\delta^{18}O$ values of daily rainfall recorded during this study (Ranichauri: -19.48‰, Jorhat: -22.79‰) were observed in September and October. On the other hand, the most positive $\delta^{18}O$ values (Jammu: +8.20 and +9.28‰) were observed towards the end of WD period (April, June). Although d-excess records shown in Fig. 3b are rather noisy, it is apparent that at Srinagar site the d-excess progressively decreases, from high d-excess values recorded in January-February ($d > 20$‰) towards low d-excess values ($d < 10$‰) recorded in September. At Jorhat, temporal evolution of the d-excess values largely coincides with that observed at Srinagar. However, during WD period, the d-excess is much more variable at this site and range from 0 to more than 40‰.

Fig.3 around here

Negative values of the d-excess were recorded from time to time at all stations of the transect (35 events in total, cf. Fig. 3, and S1b). Extreme value (-28.8‰) was recorded at Palampur station in February 2010 and was associated with very light rain (< 1 mm). As seen in Fig. 3 and S1b, largest number of events characterized by negative d-excess values was recorded at Jammu station (19 in total). Such events occurred at this site predominantly during WD period (17 out of 19 registered

cases). Negative d-excess values were observed also during Western African Monsoon (Rissi et al., 2008; Landais et al., 2010) and were generally attributed to re-evaporation of raindrops. Raindrops falling through unsaturated atmosphere below the cloud-base level undergo partial evaporation. This process was investigated in the laboratory by Steward (1975) and was modelled (e.g. Bony et al., 2008). Relative magnitude of ^{2}H and ^{18}O fractionation effects associated with evaporation process cause the evaporating water droplet to become enriched in heavy isotopes and evolve in the $\delta^{2}H$-$\delta^{18}O$ space along the line with the slope significantly lower than 8 (e.g. Rozanski et al., 2001). Thus, evaporating raindrops will move away from Local Meteoric Water Line (LMWL), eventually reaching negative d-excess values. The extent of partial evaporation is controlled mainly by relative humidity of the atmosphere through which raindrops are falling as well as by isotopic composition of ambient moisture. In fact, WD period at Jammu station is characterized by exceptionally low relative humidity (average value for WD period ca. 35%) when compared to other stations. This may explain large number of rainfall events with negative d-excess values recorded at this station.

Fig. 4 around here

Figure 4 shows daily $\delta^{2}H$ and $\delta^{18}O$ data available for Shrinagar and Jorhat stations, grouped into ISM and WD periods and plotted on $\delta^{2}H$-$\delta^{18}O$ diagram. Analogous plots for other stations are presented in the Supplement (Fig. S2). During the monsoon season the linear relationship between $\delta^{2}H$ and $\delta^{18}O$ is generally better defined, pointing to moisture sources of similar nature and similar conditions of rainfall formation. At Srinagar site, there is a striking difference between Local Meteoric Water Lines representing ISM and WD periods. The intercept of LMWL representing ISM is more than two times lower than that representing WD period, with similar slopes of both lines. Similar situation is observed for Ranichauri station. For Jorhat and Dibrugarh the seasonal differences in LMWL are less pronounced. Local Meteoric Water Lines representing WD period for Jammu and Palampur stations have significantly lower slope (5.8 and 5.5, respectively) pointing to importance of re-evaporation of raindrops at these sites outside of monsoon season (Fig. S2).

Table 3 around here

Summary isotope statistics of daily rainfall data available for all six stations, grouped into ISM and WD periods, are presented in Table 3. Arithmetic averages of three isotope parameters characterizing daily rainfall ($\delta^{2}H$, $\delta^{18}O$, d-excess) with their respective uncertainties were calculated for both periods. Arithmetic averaging was chosen in order to better reflect average conditions at moisture sources and in the regional atmosphere during the considered periods. The $\delta^{18}O$ values of daily precipitation were correlated with daily surface air temperature and rainfall amount available for each station. Linear correlations were calculated separately for ISM and WD periods. The last two columns of Table 3 summarize those calculations. Box-and-whisker plots of daily $\delta^{18}O$ and d-excess data available for each station and season are summarized in Fig. 5.

Fig. 5 around here

As seen in Table 3 and Fig. 5, ISM and WD periods are characterized by distinct isotope signatures of precipitation collected along the southern foothills of the Himalayas. Average δ^2H and $\delta^{18}O$ values for ISM period are significantly lower than those recorded for WD period at the given station. Largest difference (ca. 7.5‰ for $\delta^{18}O$ and 60‰ for δ^2H) was observed at Palampur station. Rainfall collected during ISM and WD periods differs also in the mean d-excess values. During ISM, d values are generally lower than those observed during WD period. In one case (Jammu station) this regularity is broken (very low mean d-excess for WD period). This anomalously low mean d-excess stems from large proportion of rainfall events exhibiting negative d-excess values (cf. discussion above). There is a lack of distinct spatial trends in the mean isotope characteristics of daily rainfall along the studied transect during the two seasons (cf. Fig. 5). As far as the link between $\delta^{18}O$ and local surface air temperature is concerned, positive, significant correlation was found for three stations: Srinagar (ISM period), Jammu (both periods) and Ranichauri (WD period). Significant negative correlation was observed for Jorhat and Dibrugarh stations (ISM period).

Figs. 6 & 7 around here

Distinct seasonality seen in the isotope characteristics of daily rainfall at the southern foothills of the Himalayas should be viewed in the context of large-scale seasonal changes in the circulation regime of the regional atmosphere. These changes can be best illustrated through reconstruction of back trajectories of moist air masses generating rainfall events at selected sites of the east-west transect. Backward trajectory modelling was performed for all daily precipitation events analysed in the framework of this study (548 events). Figures 6 and 7 show examples of typical backward trajectories (ensembles) representing ISM and WD periods, reconstructed for Jorhat and Srinagar stations, representative for eastern and western edge of the transect, respectively. Lower parts of Figs. 6 and 7 show evolution of selected parameters of the air parcels transported along the trajectories: (i) elevation above the local ground (m), (ii) terrain height (m a.s.l.), (iii) velocity of the air parcel (m s^{-1}), (iv) temperature of the air parcel (^oC), (v) precipitation rate (mm per 6h) and (vi) H_2O mixing ratio (g kg^{-1}). The ISM period at Jorhat station (Fig. 6a) is dominated by low-level transport of moist air masses (water vapour content of ca. 18 g kg^{-1}) from the equatorial Indian Ocean and the Bay of Bengal. The calculated ensembles have relatively low spread, reflecting large-scale, uniform movement of the moist air masses driven by monsoon circulation. The air masses reach the station from the south, without any noticeable contribution from other directions. Rainfall is generated when warm, moist air masses are lifted up over the continent and cool down from ca. 28°C to 20°C. As seen in Fig. 7a, the monsoonal air masses may reach also the Srinagar station located on the western edge of the transect. However, the ensembles shown in Fig. 7a suggest that apart from trajectories passing over the Bay of Bengal and travelling along the southern foothills of the Himalayas in the northwest direction, a more direct route of moist monsoonal air masses (water vapour content of ca. 15 g

kg^{-1}), starting in the Arabian Sea and crossing the Indian continent, is a more important source of rainfall for western Himalayas during this season. During WD period, the overwhelming majority of air masses arrive at rainfall collection stations from west and northwest directions (Figs. 6b and 7b). Typically, they travel at high elevations (4-6 thousand meters above the ground), passing the region of Black Sea and Caspian Sea, and further descend over Afghanistan and Pakistan, towards rainfall collection stations located at the western edge of the transect (Srinagar, Jammu, Palampur). These dry air masses (water vapour content around 1 g kg^{-1}) are picking up moisture of continental origin from relative proximity of the collection sites and their vapour content rises to approx. 3.5 g kg^{-1} (Fig. 7b - lower panel). For stations located at the eastern edge of the transect (Jorhat, Dibrugarh) more western routes of air masses prevail (Fig 6b). They travel east within the latitude band of 20°N to 30°N passing Arabian Peninsula, Persian Gulf, northern reaches of the Arabian Sea and northern India, gradually warming up and losing elevation. On their way east they gradually absorb moisture of both marine (Arabian Sea) and continental origin. As a result of this process, their water vapour content rises from approximately 3 g kg^{-1} at the eastern coast of the Arabian Peninsula to ca. 8 g kg^{-1} in the proximity of the eastern edge of the transect.

4.2 Evolution of $\delta^{18}O$ during ISM period

Gradual, heavy-isotope depletion of rainfall in the course of development and recession of Indian Summer Monsoon, apparent from Figs. 3a and S1, is not a local phenomenon restricted only to the studied transect. Such evolution of $\delta^{18}O$ in precipitation is observed over entire region influenced by ISM. For instance, $\delta^{18}O$ of monthly rainfall at New Delhi decreases from ca. 0‰ in June to around -9‰ in September (Araguas et al., 1998; Battacharya et al., 2003). Also the stations of IWIN programme (Deshpande and Gupta, 2008; Deshpande and Gupta, 2012) show similar effect of gradual decrease of $\delta^{18}O$ values of rainfall towards the end of ISM season in September, seen for example at Ahmedabad station in western India (Deshpande et al., 2010). The reduction of ^{18}O content of similar magnitude was observed for individual rainfall events collected during 2012 and 2013 monsoon period on Andaman Island, Bay of Bengal (Chakraborty et al., 2016).

The extent of heavy-isotope depletion of daily rainfall in the course of ISM evolution, observed in this study, is large (> 10‰ in $\delta^{18}O$). Regional thermal gradients are virtually nonexistent during ISM and hence cannot be used to explain the observed gradual reduction of $\delta^{18}O$, with sea surface temperatures in the Bay of Bengal fluctuating between 28 and 29°C (e.g. Midhun et al., 2013) and mean surface air temperatures at three low-elevation stations of the studied transect (Jammu, Jorhat, Dibrugarth) around 28°C (cf. Table 2). This gradual reduction of heavy-isotope content in precipitation is apparently a regional phenomenon inherently linked to the evolution of Indian Summer Monsoon and cannot be explained by local effects. Local effects such as enhanced convective activity in the local atmosphere and associated higher degree of rainout of moist air masses (local amount effect) or partial evaporation of raindrops, might explain short-term fluctuations of $\delta^{18}O$ visible in Figs. 3a and S1a but will not explain regional evolution of $\delta^{18}O$ and $\delta^{2}H$ values in the course of ISM. Clearly, another explanation should be considered here. In this context, it is noteworthy that Deshpande et al (2015) have shown that major moisture pickup locations for precipitation at Ahmedabad gradually change from over the Arabian sea to central Indian continental areas in the later part of ISM.

In the course of ISM period water availability on surface (lakes, reservoirs, streams, wetlands) and sub-surface (soil, vadose zone) environments and in lower atmosphere over large continental areas of India progressively increase to a substantial extent. For instance, in Assam state 9.7% of the area is at that time under wetlands including rivers, streams and riverine wetlands. The open pan annual evaporation (2.36 mm/day) and annual potential evapotranspiration (3 mm/day) at Jorhat is lowest in the country (Rao et al., 2012). The relative humidity is generally higher during summer months from June to November. The low values of open pan and potential evapotranspiration and high relative humidity in Assam suggest that atmosphere remains continuously loaded with locally generated moisture during summer months. As the monsoon progresses in India, enhanced soil moisture and vegetation cover lead to increased evapotranspiration and recycled precipitation. The recycling ratio, that is the ratio of recycled precipitation to total precipitation, is highest (around 25%) in northeast India, which has dense vegetation cover leading to high evapotranspiration. High precipitation recycling ratio was found at the end of the monsoon in the month of September (Pathak et al., 2014).

Increasing amount of moisture in the lower atmosphere in the course of ISM makes the air column unstable, prone to convective activities. In should be noted here that in absence of horizontal thermal gradients between source regions of atmospheric moisture and the continent, the principal mechanism which can generate rainfall is vertical uplift and cooling of moist air masses, associated with convective systems. If horizontal and vertical extent of convective systems increase as the monsoon progresses, it could generate the observed gradual depletion in heavy isotopes of daily rainfall in the course of ISM evolution.

Looking from a more broader perspective, a large-scale, regional recycling of moisture of oceanic origin can also contribute to the observed evolution of $\delta^{18}O$ and $\delta^{2}H$ during ISM period. Northward movement of ITCZ pulls maritime moisture from southeast Asia and the Bay of Bengal and transports it north-westward. Moist air masses are lifted by large-scale convection, loose part of their moisture content and return towards the equator as the upper branch of Hadley cell circulation. Then, they descend and mix with low-level moist air masses of oceanic origin (cf. Li et al., (2016) - Fig. 24). Descending air masses contain moisture depleted in heavy isotopes, which is then incorporated in the moist air masses of oceanic origin transported north-westward. Such regional recycling loop operating in the course of ISM evolution may provide the required mechanism for a gradual, large-scale reduction of ^{18}O and ^{2}H content in regional atmospheric moisture and precipitation during this period. Rough assessment of this effect was made assuming Rayleigh-type rainout of moist air masses of oceanic origin (RH = 80%, T = 28^{o}C), with the initial $\delta^{18}O$ value of moisture equal -10‰. It was assumed that rainout induced by large-scale convection continues down to 15% of the initial water content. Those dry air masses containing vapour depleted in heavy isotopes return as an upper branch of the recycling loop and mix with the moist air masses of oceanic origin. Five to six such recycling loops would be required to reduce the initial ^{18}O content of maritime moisture and the rainfall by approximately 10 ‰ at the end of the monsoon period, in accordance with observations.

It is likely that both mechanisms underlined above act together to produce the observed characteristic evolution of $\delta^{18}O$ and $\delta^{2}H$ in daily rainfall during ISM period. Model runs of isotope GCMs available for Indian continent (e.g. Hoffman and Heimann, 1997; Midhun and Ramesh, 2016) suggest that the models tend to underestimate the amplitude of seasonal

changes of $\delta^{18}O$, particularly in northern India. A more comprehensive isotope modelling of monsoon circulation would be needed to quantify the above-outlined mechanisms of moisture recycling and their impact on the measured stable isotope composition of precipitation in the region.

Finally, worth to comment are large seasonal changes in the isotopic composition of regional atmospheric moisture reservoir in response to contrasting circulation patterns of the regional atmosphere and moisture recycling mechanisms discussed above. When the operation of monsoon circulation engine is terminated in September, the regional atmosphere is still loaded with moisture heavily depleted in ^{2}H and ^{18}O. This remarkable heavy-isotope depletion of regional atmospheric moisture reservoir survives for several weeks. In fact, the most negative $\delta^{18}O$ value (-22.79‰) was measured in rainfall collected at Jorhat station on October 11, 2010. In the course of WD period, maritime moisture depleted in heavy isotopes is gradually replaced by moisture of continental origin characterized by elevated concentration of ^{2}H and ^{18}O (cf. discussion below). This in turn is reflected in rising δ values of rainfall in the course of WD period.

4.3 Positive $\delta^{18}O$ and $\delta^{2}H$ values of daily rainfall

Striking feature of the isotope data generated in the framework of this study is relatively frequent appearance of positive $\delta^{18}O$ and $\delta^{2}H$ values in the isotope records available for six stations collecting daily rainfall. Positive δ values range from 0.17 to 9.28‰ for $\delta^{18}O$ and from 5.3 to 56.6‰ for $\delta^{2}H$. They constitute ca. 16% of the collected and analysed data. Positive $\delta^{18}O$ and $\delta^{2}H$ values were recorded mostly during WD period (ca. 25% of all data available for this period, comparing to 5.5% recorded during ISM period). The station where positive $\delta^{18}O$ and $\delta^{2}H$ values were recorded most frequently (70% of the data available for WD period) was Jammu. To better characterize rainfall events showing positive δ values, d-excess values calculated for such events were plotted as a function of (positive) $\delta^{18}O$ values and the relative humidity of the local atmosphere (daily means). The resulting plots are shown in Fig. 8. As seen in Fig. 8, d-excess values decrease with increasing $\delta^{18}O$ values (R^2=0.349) and increase with rising relative humidity (RH) of the local atmosphere (R^2=0.147). In a comprehensive study of West African Monsoon precipitation near Niamey, Niger (Landais et al., 2010) significantly higher slope of d-excess - RH correlation was found (0.38), when compared to that characterizing data points shown in the lower panel of Fig. 8 (0.22 ± 0.05). Also the variables were much better correlated (R^2=0.68, Fig. 7b in Landais te al., 2010). This is, however, not surprising, keeping in mind that the data reported by Landais et al., (2010) were originating from one station (Banbizoumbou) and were restricted to the monsoon season only (June - September) whereas the data shown in Fig.8 cover both seasons (ISM and WD) and represent six stations distributed along the 2900 km transect along southern foots of the Himalayas. Moreover, relative humidity data in Landais et al., (2010) study were reconstructed mean RH values for the lower troposphere (200 - 1000 m a.g.l) wheres in our case we used daily means of RH values measured near the ground level.

Fig. 8 around here

The ^{18}O isotope composition of maritime moisture collected onboard a ship (mast top, ca. 25 m above sea level) cruising the Bay of Bengal during the ISM period (from July 13 till August 3, 2012) varied between ca. -10 and -14‰ (Midhun et al., 2013). If one adopts -10‰ as representative $\delta^{18}O$ value for unaltered oceanic moisture from which monsoon precipitation is formed, and assuming further that this moisture is transported towards the southern foothills of the Himalayas without any noticeable rainout effect, the expected $\delta^{18}O$ value of the first condensate would be around -1.0 ‰. It is highly unlikely that unaltered maritime moisture can reach such remote continental sites as Jammu station where positive δ values are most common. Hence, the 'first condensate' scenario cannot fully explain positive $\delta^{18}O$ and $\delta^{2}H$ values recorded at the stations along the transect, even if partial evaporation of raindrops on their way to the ground is considered.

As the majority of positive δ values was recorded during WD period, the explanation of positive $\delta^{18}O$ and $\delta^{2}H$ values should involve sources of moisture other than oceanic ones. One can distinguish three components of backward flux of water into the regional atmosphere over the continental areas, each characterized by distinct isotope signature: (i) water transpired by plant cover, (ii) water evaporated from bare soil, and (iii) water evaporated from surface water bodies. It is a well-established fact that in the course of transpiration process, leaf water is becoming progressively enriched in heavy stable isotopes, quickly reaching hydrologic and isotopic steady-state (e.g. Dongmann et al., 1974; Flanagan et al., 1991). Under such conditions, the isotopic composition of water vapour released into the atmosphere is isotopically identical with the source water utilized by plants. In our case the water utilized by plants originates predominantly from rainy (monsoon) season. The amount-weighted mean $\delta^{18}O$ of ISM precipitation for three low-altitude stations (Jammu, Dibrugarh, Jorhat) is -6.5‰. First condensate produced from such water vapour (assumed condensation temperature of $+10^{o}C$) will be characterized by $\delta^{18}O$ values close to +4.2‰, which falls within the range of positive δ values of daily rainfall collected at the stations. Soil water evaporation may also produce water vapour, the isotopic composition of which is identical to that of the source (soil) water. However, due to much larger size of soil water reservoir when compared to leaf water, establishing steady-state isotope evaporation profile in the soil column requires much longer periods of time than is the case of leaf water reservoir (weeks instead of hours). This is possible only under arid or semi-arid conditions, with periods between consecutive rain events long enough (e.g. Zimmerman et al., 1966; Barnes et al., 1983) and is generally not the case for the study area. Evaporation from bare soil will resembles in this case evaporation from open water bodies. Isotopic composition of evaporating surface water bodies evolve in the $\delta^{2}H$-$\delta^{18}O$ space along the so-called local evaporation line with the slope significantly lower than 8 (e.g. Gat, 1996). The mass balance considerations require that water vapour being released into the local atmosphere in the course of such process is located on the local evaporation line, to the left-hand side of the local meteoric water line (LMWL). This water vapour has somewhat reduced heavy isotope content when compared to the source water subject to evaporation and is characterized by high deuterium excess (e.g. Rozanski et al., 2001).

All three processes outlined above are most probably acting together under climatic conditions characteristic for the studied region and are apparently capable of delivering sufficient amounts of moisture to the regional atmosphere to produce rainfall characterized by positive δ values, even at locations which are far away from oceanic sources of water. It is likely that generally higher and more variable d-excess values of rainfall events recorded in the course of WD period (cf. Figs. 3a and S1a), reflects varying contribution of those three processes to the backward flux of moisture into the regional atmosphere, generated by Indian subcontinent during that period of the year. The fact that d-excess values are inversely correlated with $\delta^{18}O$ and increase with rising relative humidity of near-ground atmosphere (cf. Fig. 8), point to partial evaporation of raindrops as an additional mechanism contributing to the observed range of positive $\delta^{18}O$ and $\delta^{2}H$ values.

4.4 Significance of elevated d-excess values

Higher than the global average d-excess value (ca. 10‰) in meteoric waters originating from the Himalayas and Tibetan Plateau was often used to infer Mediterranean or more generally westerly derived vapour (Tian et al 2005; Hren et al., 2009; Jeelani et al., 2010; Bershaw et al., 2012). The observed high d-excess in rainfall was generally related to higher d-excess (ca. 20‰) found in the vapour generated over east Mediterranean Sea (Gat and Carmi, 1970). Here we argue that these high d-excess values recorded in the Himalayas do not necessarily originate from the Mediterranean Sea. There were 38 rainfall events with d > 20‰ observed in this study (ca. 6.9% of all events analysed). Higher d-excess values occurred mostly during WD period (31 out of 38 cases). However, the highest d values were recorded during ISM period (Jammu, 34.0 and 39.1‰; Jorhat, 40.7 and 44.0‰).

Largest number of events characterized by high d-excess values was recorded at Srinagar station during WD period (21 out of 90 analysed for this period). The only station without elevated d-excess values was Dibrugarh. Closer examination of backward trajectory ensembles calculated for days with high d-excess values reveal that trajectories associated with daily rainfall samples characterized by high d-excess values arrive at Srinagar from northwest, west or southwest. However, as discussed above, those air masses are generally very dry and pick-up moisture of continental origin only in relative proximity of rainfall collection stations (cf. Fig. 7b). Surprisingly, high d-excess values recorded at Jammu station are almost exclusively associated with characteristic monsoon-type circulation (Fig. S3) . In one case, recorded during WD period (31/12/2010), the air masses were circling around over the Indian subcontinent, interacting strongly with the surface.

Common feature of almost all trajectories at all the precipitation sites with high d-excess is their long residence time in relative proximity of the sampling site, as illustrated in Fig. S4 for Jorhat station. Apparently, this leaves enough time for their prolonged interaction with the surface in which evaporation of surface water bodies (lakes, swamps, etc.) and/or non-steady-state evaporation of soil moisture serve as important sources of water vapour characterized by high d-excess values. Rainfall produced from such vapour will retain this characteristic isotope signature in the form of high d-excess value. Some impact of atmospheric moisture with high d-excess arriving from Eastern Mediterranean in the Himalayan region is certainly possible, although in our opinion is rather unlikely that this is an important source of rainfall in the region. Low-level eastward moving, turbulent transport of moisture from Eastern Mediterranean towards the Himalayas will be inevitably

associated with strong interaction with the surface on the way (rainfall, backward moisture fluxes) which will blur the original isotope signature of the moisture of marine origin.

4.5 Footprint analysis

To better characterize the contribution of different air masses arriving in the course of ISM and WD seasons at six stations collecting daily rainfall along southern foothills of the Himalayas, footprint analysis was performed. Footprint maps were calculated for 2009-2011 period, based on daily simulations of 10-day long backward trajectories, started at each of the locations at noon local time. Footprint maps were prepared for three stations (Jammu, Kathmandu and Jorhat) representing western, central and eastern part of the studied transect, respectively. Separate maps were constructed for ISM and WD periods and are presented in Fig.9. The maps shown in Fig. 9 provide a valuable insight into great seasonal contrast in the circulation patterns of the regional atmosphere, which in turn control rainfall regime in the region (amount, its seasonal distribution and stable isotope composition).

Fig. 9 around here

The footprint map representing ISM period at Jorhat station clearly demonstrates overwhelming dominance of monsoon circulation bringing moisture-loaded air masses from tropical Indian Ocean and Bay of Bengal towards the eastern region of the Himalayas. There is a very small contribution (in the order of few percent) of the air masses arriving from west and northwest. Dominating influence of monsoon air masses is seen also in the central portion of the transect (Kathmandu site), although the presence of air masses originating in the Arabian Sea and crossing Indian subcontinent in the northeast direction is also noticeable. The footprint map for Jammu station representing western Himalayas clearly shows three major types of air masses arriving at this site during ISM period: (i) maritime monsoonal air masses originating in the Bay of Bengal and travelling along southern foothills of the Himalayas, (ii) continental air masses coming from northwest direction, and (iii) the air masses originating in the Arabian Sea and travelling along India-Pakistani border towards eastern Himalayas, the first being the dominating component.

During WD period, the circulation patterns of regional atmosphere change radically. The Jorhat station receives air masses predominantly from northern India and Pakistan, with noticeable contribution from the Bay of Bengal. The footprint map is generally more diffuse, indicating presence of continental air masses with the origin in central Asia as well as Black Sea and Caspian Sea region. Similar picture is observed for Kathmandu station, with majority of air masses coming from northern India and Pakistan. The impact of maritime air masses (Bay of Bengal) is reduced, although still visible. The western part of the Himalaya (Jammu station) is under overwhelming influence of air masses coming from the west (Iran, Iraq, Afghanistan and Pakistan). Whereas small contribution of oceanic air masses coming from eastern Arabian Sea is still visible, air masses coming from the Bay of Bengal are practically absent.

6. Conclusions

Isotope analyses of daily precipitation samples collected at six stations located along the southern foothills of the Himalayas allowed a deeper insight into the mechanisms controlling isotopic composition of precipitation in this important region of Indian subcontinent. Analysis of ^{2}H and ^{18}O isotope composition of daily precipitation, combined with extensive backward trajectory modelling of the air masses associated with rainfall in the studied region, allowed several important conclusions to be drawn with respect to origin of atmospheric moisture and precipitation in two contrasting seasons (Indian Summer Monsoon and Western Disturbances).

It is suggested that gradual reduction in ^{2}H and ^{18}O content of precipitation in the region, progressing from positive $\delta^{18}O$ values, down to less than -10‰ in the course of ISM evolution, stems from convective activities in the regional atmosphere and large-scale recycling of moisture of oceanic origin, driven by monsoonal circulation. Superimposed on this general trend are short-term fluctuations of the isotopic composition of rainfall which might have their roots in local effects such as locally enhanced convective activity and associated higher degree of rainout of moist air masses (local amount effect), partial evaporation of raindrops or impact of isotopically heavy moisture generated in evapotranspiration processes taking place in the vicinity of rainfall sampling sites. Seasonal footprint maps constructed for three stations representing western, central and eastern portion of the Himalayan region indicate that the influence of monsoonal circulation reaches western edges of the Himalayan region. While characteristic imprint of monsoon air masses (increase of monthly rainfall amount) can be completely absent in eastern Himalaya, the onset of ISM period is still clearly visible in the isotopic composition of individual precipitation events.

The most characteristic feature of daily precipitation collected in the studied region during WD period is its relatively high ^{2}H and ^{18}O content when compared to ISM period, and the presence of large number of daily rainfall samples exhibiting positive $\delta^{18}O$ and $\delta^{2}H$ values. These peculiar isotope characteristics can be explained only when dominating continental origin of the source moisture for this precipitation is postulated. Water stored in the soil during ISM period is returned to the regional atmosphere during WD period through evapotranspiration processes. Backward trajectory modelling has shown that long-range transport of air masses from the west and northwest, characteristic for WD period, occurs at high elevations and cannot bring sufficient amounts of moisture to contribute significantly to precipitation in the study area during this period. Instead, the major supply of moisture for rainfall during WD period is mainly of local (regional) origin, stemming from transpiration of plant cover, soil water evaporation and evaporation of surface water bodies. All these processes deliver water vapour, which is significantly enriched in heavy isotopes compared to unaltered vapour of oceanic origin. This enrichment is then reflected in the isotopic composition of rainfall produced from such vapour. Isotope characteristics of rainfall during WD period are consistent with this scenario. Seasonal footprint maps show that during that period eastward moving air masses may reach the eastern edges of the Himalayas. Footprint maps also suggest that some presence of air masses coming from the Bay of Bengal and bringing moisture of oceanic origin to the study area cannot be excluded.

It appears that high d-excess values of daily rainfall collected along southern foothills of the Himalayas can be associated with air masses of very different origin. However, the common feature of almost all such cases is relatively long interaction of air masses with the continental surface, providing a chance to accommodate enough moisture of continental origin, characterized by elevated d-excess values, which then is transferred to the local rainfall.

6. Data availability

All the isotope data used in this manuscript can be requested from R.D. Deshpande at desh@prl.res.in. Backward trajectory modelling was done for all daily precipitation events analysed in the framework of this study. The modelling results as well as the data used to construct footprint maps are available on request from M. Galkowski (Michal.Galkowski@fis.agh.edu.pl).

7. Authors contribution

G. Jeelani drafted the manuscript with the inputs from R.D. Deshpande, M. Galkowski and K. Rozanski. All the authors reviewed the manuscript and interpreted the data. M. Galkowski conducted Hysplit modelling.

8. Competing interests

The authors declare that they have no conflict of interest

9. Acknowledgements

Part of the sampling and the isotope analyses discussed in this study was undertaken under the aegis of IWIN National Programme (Deshpande and Gupta, 2008) funded jointly by the Department of Science and Technology (DST), Govt. of India, vide Grant No. IR/ S4/ESF-05/2004 and the Physical Research Laboratory (PRL). Authors acknowledge support of DST and PRL with gratitude. The IMD and CRIDA collected the rainwater samples from some of the stations included in this study. M. Galkowski and K. Rozanski were supported by the statutory funds of the AGH University of Science and Technology (project no. 11.11.220.01/1). We appreciate constructive comments by one anonymous reviewer and M. Schulz, Co-Editor of ACP. They helped us to improve considerably the manuscript.

10. References

Agnihotri, C.L. and Singh, M. S.: Satellite study of western disturbances, Mausam, 33, 249-254,1982.

Allan, R.P. and Soden, B. J.: Atmospheric warming and the amplification of precipitation extremes, Science, 321, 1481-1484, 2008.

Allen, M.B. and Armstrong, H. A.: Reconciling the Intertropical Convergence Zone, Himalayan/Tibetan tectonics, and the onset of the Asian monsoon system, J. Asian Earth Sci., 44, 36-47, 2012.

Araguás-Araguás, L., Froehlich, K. and Rozanski, K.: Deuterium and oxygen-18 isotope composition of precipitation and atmospheric moisture, Hydrol. Processes, 14, 1341-1355, 2000.

Araguás-Araguás, L., Froehlich, K. and Rozanski, K.: Stable isotope composition of precipitation over Southeast Asia, J. Geophys. Res., 103, 28721-28742, 1998.

Archer, D.R., Forsythe, N., Fowler, H.J. and Shah, S.M.: Sustainability of water resources management in the Indus Basin under changing climatic and socio economic conditions, Hydrol. Earth Syst. Sci., 14, 1669-1680, 2010.

Barnes, C.J. and Allison, G.B.: The distribution of deuterium and O-18 in dry soils. 1. Theory, J. Hydrol., 60, 141-156, 1983.

Bershaw, J., Penny, S.M. and Garzione, C.N.: Stable isotopes of modern water across the Himalaya and eastern Tibetan Plateau: Implications for estimates of paleoelevation and paleoclimate, Journal of Geophysical Research: Atmospheres, 117D2, 2012.

Bhattacharya, S.K., Froehlich, K., Aggarwal, P.K. and Kulkarni, K.M.: Isotopic variation in Indian Monsoon precipitation: records from Bombay and New Delhi, Geophys. Res. Lett., 30(24), 2285, 2003.

Bony, S., Rissi, C. and Vimeux, F.: Influence of convective processess on the isotopic composition ($\delta^{18}O$ and δD) of precipitation and water vapour in the tropics: 1. Radiative-convective equilibrium and Tropical Ocean-Global Atmosphere-Coupled Ocean_Atmosphere Response Experiment (TOGA-COARE) simulations, J. Geophys. Res. 113, D19305, 2008.

Bookhagen, B. and Burbank, D. W.: Toward a complete Himalayan hydrological budget: spatiotemporal distribution of snowmelt and rainfall and their impact on river discharge, J. Geophys. Res., 115, F03019, 2010.

Breitenbach, S. F. M., Adkins, J. F., Meyer, H., Marwan, N., Kumar, K.K., and Haug, G. H.: Strong influence of water vapour source dynamics on stable isotopes in precipitation observed in southern Meghalaya, NE India, Earth Planet. Sci., Lett., 292 212–220, 2010.

Cannon, F., Carvalho, L.M.V., Jones, C. and Bookhagen, B.: Multi-annual variations in winter westerly disturbance activity affecting the Himalaya, Clim. Dyn., 44, 441-455, 2015.

Chakraborty, S., Sinha, N., Chattopadhyay, R., Sengupta, S., Mohan, P.M. and Datye, A.: Atmospheric controls on the precipitation isotopes over the Andaman Islands, Bay of Bengal, Scientific Reports, 6, 19555, doi:10.1038/srep19555, 2016.

Chand, R. and Singh, C.: Movement of Western Disturbances and associated cloud convection, J. Ind. Geophys. Union, 19, 62-70, 2015.

Clemens, S., Prell, W., Murray, D., Shimmield, G. and Weedon, G.: Forcing mechanisms of the Indian Ocean monsoon, Nature, 353, 720-725, 1991.

Craig, H.: Isotope variations in meteoric waters, Science, 133, 1702-1703, 1961.

Dansgaard, W.: Stable isotopes in precipitation, Tellus, 16, 436-468, 1964.

Deshpande, R.D. and Gupta, S.K.: Oxygen and hydrogen isotopes in hydrological cycle: New data from IWIN national programme, Proceedings Indian National Science Academy, 78, 321-331, 2012.

Deshpande, R.D. and Gupta, S.K.: National programme on isotope fingerprinting of waters of India (IWIN). Glimpses of Geosciences Research in India, the Indian Report to IUGS, Indian National Science Academy. 10-16, 2008.

Deshpande, R.D., Maurya, A.S., Kumar, B., Sarkar, A. and Gupta, S.K.: Rain-vapor interaction and vapor source identification using stable isotopes from semi-arid Western India, J. Geophys. Res., 115, D23311, 2010.

Deshpande, R.D., M. Dave, V. Padhya, H. Kumar and Gupta, S.K.: Water vapour source identification for daily rain events at Ahmedabad in semi-arid western India: wind trajectory analyses, Meteorological Applications, 22, 754-762, 2015.

Dhar, O.N., Kulkarni, A.K. and Sangam, E.B.: Some aspects of winter & monsoon rainfall distribution over the Garhwal-Kumaon Himalaya: a brief appraisal, Himal. Res. Dev., 2, 10-19, 1984.

Dimri, A.P.: Surface and upper air fields during extreme winter precipitation over the western Himalayas, Pure Appl. Geophys., 163, 1679-1698, 2006.

Dimri, A.P., Mohanty, U.C. and Mandal, M.: Simulation of heavy precipitation associated with an intense western disturbance over Western Himalayas, Nat. Hazards, **31**, 499-521, 2004.

Dimri, A.P., Niyogi, D. Barros A.P., Ridley, J., Mohanty U.C., Yasunari, T. and Sikka, D.R.: Western Disturbances: A review, Reviews of Geophysics, 53, 225-246, 2015.

Dongmann, G., Nurnberg, H.W. Förstel, H. and Wagener, K.: On the enrichment of $H_2^{18}O$ in the leaves of transpiring plants, Radiation and Environmental Biophysics, 11, 41-52, 1974.

Flanagan, L.B., Marshall, J.D. and Ehleringer, J.R.: Comparison of modelled and observed environmental influences on the stable oxygen and hydrogen isotope composition of leaf water in *Phaseolus vulgaris L,* Plant Physiology, 96, 623-631, 1991.

Gadgil, S.: The Indian monsoon and its variability, An. Rev. Earth Planet. Sci., 31, 429-467, 2003.

Gat, J.R.: Oxygen and hydrogen isotopes in the hydrologic cycle, An. Rev. Earth Planet. Sci., 24, 225-262, 1996.

Gat, J.R. and Carmi, I.: Evolution of the isotopic composition of atmospheric waters in the Mediterranean Sea area, J. Geophys. Res., 75, 3039-3048, 1970.

Held, I.M. and Soden B.J.: Robust response of the hydrological cycle to global warming, J. Clim., 19, 5686-5699, 2006.

Hren, M.T., Bookhagen, B., Blisniuk, P.M., Booth, A.L. and Chamberlain, C.P.: $\delta^{18}O$ and δD of streamwater across Himalayan and Tibetan Plateau: Implications for moisture sources and palaelevation studies. Earth Planet. Sci. Lett., 288, 20-32, 2009.

Hoffmann, G. and Heimann, M.: Water isotope modelling in the Asian monsoon region, Quaternary International, 37, 115-128, 1997.

IPCC, Climate Change 2013: The Physical Science Basis. Contribution of Working Group I to the Fifth Assessment Report of the Intergovernmental Panel on Climate Change edited by T. F. Stocker, D. Qin, G.-K. Plattner, M. Tignor, S.K. Allen, J. Boschung, A. Nauels, Y. Xia, V. Bex and P.M. Midgley, Cambridge University Press, Cambridge, United Kingdom and New York, NY, USA, 1535 pp, doi:10.1017/CBO9781107415324, 2013.

Ives, J.D. and Messerli, B.: The Himalayan Dilemma: Reconciling Development and Conservation, John Wiley, London, doi:10.4324/9780203169193, 1989.

Jeelani, G., Faddema, J., Van der Veen, C. and Leigh, S.: Role of snow and glacier melt in controlling river hydrology in Liddar watershed (western Himalaya), Water Resour. Res., 48, W12508, 2012.

Jeelani, G., Kumar, U.S., Bhat, N.A., Kumar, B., Sharma, S.: Variation of $\delta^{18}O$, δD and ^3H in karst springs of south Kashmir, western Himalayas (India), Hydrol., Proces., 29, 522-530, 2015.

Jeelani, G. and Deshpande, R.D.: Isotope fingerprinting of precipitation associated with western disturbances and Indian summer monsoons across the Himalayas, Journal of Earth System Science, 126(8), p.108, 2017.

Jeelani, G., Shah, R. A., Deshpande, R. D., Fryer, A., Perrin, J., Mukherjee, A.: Distinguishing and estimating recharge to karst springs in snow and glacier dominated mountainous basins of the western Himalaya, India, Journal of Hydrology, 550, 239-252, 2017a.

Jeelani, G., Deshpande, R. D., Shah, R.A., Hassan, W.: Influence of southwest monsoons in Kashmir Valley, Western Himalaya, Isotopes in Environment and Health Studies, 53(4), 400-412, 2017b.

Karim, A. and Veizer, J.: Water balance of the Indus River Basin and moisture source in the Karakoram and western Himalayas: Implications from hydrogen and oxygen isotopes in river water, J. Geophys. Res. Atmos., 107, 4362, 2002.

Kendall, C. and Coplen, T.B.: Distribution of oxygen-18 and deuterium in river waters across the United States, Hydrol. Processes, 15, 1363-1393, 2001.

Kumar, B., Rai, S. P., Kumar, U. S., Verma, S, K., Garg, P., Kumar, S. V. V., Jaiswal, R., Purendra, B, K., Kumar, S. R. and Pande, N. G.: Isotopic characteristics of Indian precipitation, Water Resour. Res., 46, 1-15, 2010.

Landais A., Rissi, C., Bony, S., Vimeux, F., Descroix, L., Falourd, S., and Bouygues, A.: Combined measurements of $^{17}O_{excess}$ and d-excess in African monsoon precipitation: Implications for evaluating convective parameterizations. Earth and Planetary Science Letters, Volume 298, 104-112, 2010.

Lang, T.J. and Barros, A.P.: Winter storms in the central Himalayas, J. Meteor. Soc. Jpn., 82, 829-844, 2004.

Lekshmy, P.R., Midhun, M. and Ramesh, R.: Spatial variation of amount effect over peninsular India and Sri Lanka: role of seasonality, Geophys. Res. Lett., 42, doi:10.1002/2015GL064517, 2015 .

Lekshmy, P. R., Midhun, M., Ramesh, R. and Jani, R.A.: ^{18}O depletion in monsoon rain relates to large scale organized convection rather than the amount of rainfall, Scientific Reports, 4, doi:10.1038/srep05661, 2014.

Li, Z., Lau, W.K.-M., Ramanathan, V., Wu, G., Ding, Y., Manoj, M.G., Liu, J., Qian, Y., Li, J., Zhou, T., Fan, J., Rosenfeld, D., Ming, Y., Wang, Y., Huang, J., Wang, B., Xu, X., Lee, S.-S., Cribb, M., Zhang, F., Yang, X., Zhao, Z., Takemura, T., Wang, K., Xia, X. Yin, Y., Zhang, H., Gou, J., Zhai, P.M., Sugimoto, N., Babu, S.S. and Brasseur, G.P.: Aerosol and monsoon climate interactions in Asia, Reviews in Geophys., 54, doi:10.1002/2015RG000500, 2016.

Madhura, R.K., Krishnan, R., Revadekar, J.V., Mujumdar, M. and Goswami, B.N.: Changes in western disturbances over the Western Himalayas in a warming environment. Clim. Dyn., 44, 1157-1168, 2015.

Maharana, P. and Dimri, A.P.: Study of seasonal climatology and interannual variability over India and its sub-regions using a regional climate model (RegCM3), Earth Sys. Sci., 123, 1147-1169, 2014.

Maurya, A.S., Shah, M., Deshpande, R.D., Bhardwaj, R.M., Prasad, A. and Gupta, S.K.: Hydrograph separation and precipitation source identification using stable water isotopes and conductivity: River Ganga at Himalayan foothills, Hydrol. Processes, 25, 1521-1530, 2011.

Maurya, A.S., Shah, M., Deshpande, R.D. and Gupta, S.K.: Protocol for $\delta^{18}O$ and δD analyses of water sample using Delta V plus IRMS in CF Mode with Gas Bench II for IWIN National Programme at PRL, Ahmedabad, Proceedings of the 11th

ISMAS Triennial Conference of Indian Society for Mass Spectrometry, Hyderabad, Indian Society for Mass Spectrometry, Mumbai, 314-317, 2009.

Molnar, P., Boos, W.R. and Battisti, D.S.: Orographic controls on climate and paleoclimate of Asia: thermal and mechanical roles for the Tibetan Plateau, An. Rev. Earth Planet. Sci., 38, 77, 2010.

Midhun, M., Lekshmy, P.R. and Ramesh, R.: Hydrogen and oxygen isotopic compositions of water vapor over the Bay of Bengal during monsoon, Geophys. Res. Lett., 40, 6324-6328, 2013.

Midhun, M., Ramesh, R.: Validation of $\delta^{18}O$ as a proxy for past monsoon rain by multi-GCM simulations, Clim. Dyn., 46, 1371-1385, 2016.

Mooley, D.A.: The role of western disturbances in the production of weather over India during different seasons, Ind. J. Meteorol. Geophys., 8, 253-260, 1957.

Overpeck, J., Anderson, D., Trumbore, S. and Prell, W.: The southwest Indian Monsoon over the last 18,000 years, Clim. Dyn., 12, 213-225, 1996.

Parrish, D. F. and Derber, J. C.: The National Meteorological Center's Spectral Statistical-Interpolation Analysis System, Mon. Weather Rev., 120, 1747-1763, doi: 10.1175/1520-0493(1992)120<1747:TNMCSS>2.0.CO;2, 1992.

Pathak, A., Ghosh S. and Kumar, P.: Precipitation recycling in the Indian subcontinent during summer monsoon, J. Hydromet., 15, 2050-2066, 2014.

Pisharoty, P.R. and Desai, B.N.: Western disturbances and Indian weather, Ind. J. Meteorol. Geophys., 8, 333-338, 1956.

Rao, Y. P. and Srinivasan, V.: Forecasting Manual, Part II Discussion of typical synoptic weather situation: winter western disturbances and their associated features, Ind. Meteorol. Depart., FMU, Report No. III-1, 1969.

Rao, B. B., Sandeep, V.M., Rao, V.U.M. and Venkateswarlu, B.: Potential evapotranspiration estimation for Indian conditions: Improving accuracy through calibration coefficients, Tech. Bull., 1, 2012.

Risi, C., Bony, S., Vimeux, F., Descroix, L., Ibrahim, B., Lebreton, E., Mamadou, I., and Sultan, B.: What controls the isotopic composition of the African monsoon precipitation? Insights from event-based precipitation collected during the 2006 AMMA field campaign, Geophys. Res. Lett., 35, L24808, 2008.

Rozanski, K., Sonntag, C. and Münnich, K.O.: Factors controlling stable isotope composition of European precipitation, Tellus, 34, 142–150, 1982.

Rozanski, K., Araguás-Araguás, L. and Gonfiantini, R.: Isotopic patterns in modern global precipitation. In: Climate Change in Continental Isotopic Records, Geophysical Monograph 78, American Geophysical Union, Washington D.C., 1-36, 1993.

Rozanski, K., Froehlich, K., and Mook, W.G.: Surface water. In: Environmental Isotopes in the Hydrological Cycle, Vol. III, Technical Documents in Hydrology, No. 39, UNESCO, IAEA, 117pp., 2001.

Siegenthaler, U. and Oeschger, H.: Correlation of ^{18}O in precipitation with temperature and altitude, Nature, 285, 314-317, 1980.

Steward, M.K.: Stable isotope fractionation due to evaporation and isotopic exchange of falling waterdrops: applications to atmospheric processes and evaporation of lakes, J. Geophys. Res. 80, 1133-1146, 1975.

Stein, A.F., Draxler, R.R., Rolf, G.D., Stundler, B.J.B., Cohen, M.D. and Ngan, F.: NOAA's HYSPLIT atmospheric transport and dispersion modeling system, Bull. Amer. Meteor. Soc., 96, 2059-2077, 2015.

Tian L., Tandong, Y., White, J.W.C., Wusheng, Y., and Ninglian, W.: Westerly moisture transport to the middle of Himalayas revealed from the high deuterium excess, Chinese Science Bulletin, **50**, 1026-1030, 2005.

Tiwari, V.M., Wahr, J. and Swenson, S.: Dwindling groundwater resources in northern India from satellite gravity observations. Geophys. Res. Lett., 36, L18401, 2009.

Upadhyay, R.G., Ranjan, R. and Negi, P.S.: Climatic variability and trend at Ranichauri (Uttarakhand), Journal of Agrometeorology, 17, 241-243, 2015.

Warrier, C.U., Babu, M.P., Manjula, P., Velayudhan, K.T., Hameed, S.A. and Vasu, K.: Isotopic characterization of dual monsoon precipitation: evidence from Kerala, India, Curr. Sci., 98, 1487-1495, 2010.

Wentz, F.J., Ricciardulli, L. and Hilburn, K.: How much more rain will global warming bring, Science, 317, 233-235, 2007.

Yadava, M. G., Ramesh, R., and Pandarinath, K.: A positive amount effect in the Sahayadri (Western Ghats) rainfall. Current Science, 93, 4, 560-564, 2007.

Yurtsever, Y., and Gat, J.: Atmospheric waters. In: Stable isotope hydrology: Deuterium and oxygen-18 in the water cycle. edited by J. R. Gat, and R. Gonfiantini, IAEA, Vienna, Austria, 103-142, 1981.

Zimmermann, U., Ehhalt, D.H. and Münnich, K.O.: Soil water movement and evapotranspiration: changes in the isotopic composition of water, Isotopes in Hydrology, IAEA, Vienna, Austria, 567-584, 1967.

Table 1. General characteristics of the stations collecting daily precipitation samples for isotope analyses.

Station code	Station name	Latitude/ Longitude	Altitude (m a.s.l.)	Mean annual temperature (^{o}C)	Mean annual precipitation (mm)	Sampling period	Analysed rainfall events
SGR	Srinagar	34°04´59"N/ 74°47'50"E	1595	13.6	693	04-2010/ 09-2011	121
JMU	Jammu	32°39'22"N/ 74°48'04"E	267	24.2	1238	07-2009/ 06-2011	98
PMR	Palampur	32°06'01"N/ 76°32'49"E	1275	19.1	2493	09-2008/ 09-2010	31
RNC	Ranichauri	30°18'50"N/ 78°24'25"E	1872	15.1	1272	02-2009/ 12-2010	31
JRH	Jorhat	26°43'21"N/ 94°11'44"E	99	24.0	2324	02-2010/ 12-2011	242
DBR	Dibrugarh	27°29'05"N/ 95°01'18"E	111	23.2	2781	06-2009/ 10-2010	25

Table 2. Long-term (1985-2014) characteristics of surface air temperature and precipitation for Indian Summer Monsoon (ISM) and Western Disturbances (WD) periods, for the stations collecting daily precipitation samples for isotope analyses. Source of data: Srinagar, Jammu, Palampur, Jorhat, Dibrugarh - pl.climate-data.org; Ranichauri - Upadhyay et al., (2015).

Station	Duration of ISM*)	A_T**) (°C)	ISM period		WD period		R***)
			T (°C)	P (mm)	T (°C)	P (mm)	
Srinagar	July-Sept.	23.1	23.0	150	10.5	543	0.28
Jammu	July-Sept.	21.0	29.7	854	22.4	384	2.22
Palampur	July-Sept.	17.2	23.2	1772	15.6	721	2.46
Ranichauri	June-Sept.	14.4	20.5	842	12.4	431	1.95
Jorhat	May-Sept.	12.3	28.1	1759	21.0	565	3.11
Dibrugarh	May-Sept.	11.7	27.1	2151	20.5	630	3.41

*) - onset and duration of ISM period defined operationally on the basis of seasonal distribution of long-term monthly rainfall (cf. Fig. 2) and through examination of individual backward trajectories calculated for daily rainfall events collected by each station in the framework of the present study.

**) - peak-to-peak amplitude of long-term (1985-2014) seasonal changes of monthly surface air temperature at the station.

***) - the ratio of cumulative rainfall amount collected at the given station during ISM and DW periods.

Table 3. Mean isotope characteristics of daily precipitation collected at six stations along southern foothills of the Himalayas, calculated for Indian Summer Monsoon (ISM) and Western Disturbances (WD) periods. Slopes of the best fit lines approximating the relationship between surface air temperature ($\Delta\delta^{18}O/\Delta T$) and precipitation amount (($\Delta\delta^{18}O/\Delta P$), based on daily data available for each period, are reported in the last two columns of the table.

Station	Period*	$\delta^{18}O$ (‰)	$\delta^{2}H$ (‰)	d-excess (‰)	N**	$(\Delta\delta^{18}O/\Delta T)$***	$(\Delta\delta^{18}O/\Delta P)$***
Srinagar	ISM	-5.81±0.79	-42.6±5.8	3.9±1.6	31	+	+ –
	WD	-4.19±0.48	-17.2±3.7	16.3±0.8	90	+ –	–
Jammu	ISM	-5.34±0.63	-30.9±4.6	11.5±1.1	51	+	+ –
	WD	1.94±0.58	17.3±3.6	1.8±1.8	47	+	+ –
Palampur	ISM	-8.70±2.51	-60.9±17.6	8.7±2.5	12	+ –	+ –
	WD	-1.24±0.28	-0.7±0.2	11.3±1.4	19	+ –	+ –
Ranichauri	ISM	-8.96±2.11	-60.8±14.3	10.8±2.5	18	+ –	+ –
	WD	-2.16±0.58	-4.1±1.1	13.2±3.5	13	+	+ –
Jorhat	ISM	-6.88±0.52	-43.3±3.3	11.7±0.9	172	+ –	+ –
	WD	-1.99±0.24	-2.2±0.3	13.8±1.6	70	–	+ –
Dibrugarh	ISM	-6.64±1.65	-40.2±10.1	12.9±3.2	16	–	n.d.
	WD	-1.92±0.64	-4.5±1.5	10.9±3.6	9	+ –	n.d.

*) - onset and duration of Indian Summer Monsoon (ISM) period defined operationally on the basis of seasonal distribution of long-term monthly rainfall (cf. Fig. 2) and through examination of individual backward trajectories calculated for daily rainfall data collected by each station in the framework of the present study. Duration of ISM for Srinagar, Jammu and Palampur: July-September; for Ranichauri: June-September; for Jorhat and Dibrugarh: May-September. Rest of the year defined as Western Disturbances (WD).

**) - number of daily precipitation samples analysed

***) - ' + ' sign signifies positive, significant ($R \geq 0.4$) correlation between $\delta^{18}O$ and daily temperature or precipitation.
' – ' sign signifies negative, significant ($R \geq 0.4$) correlation between $\delta^{18}O$ and daily temperature or precipitation.
' + – ' sign signifies lack of significant ($R \geq 0.4$) correlation between $\delta^{18}O$ and daily temperature or precipitation.

n.d. - not determined

Figure Captions

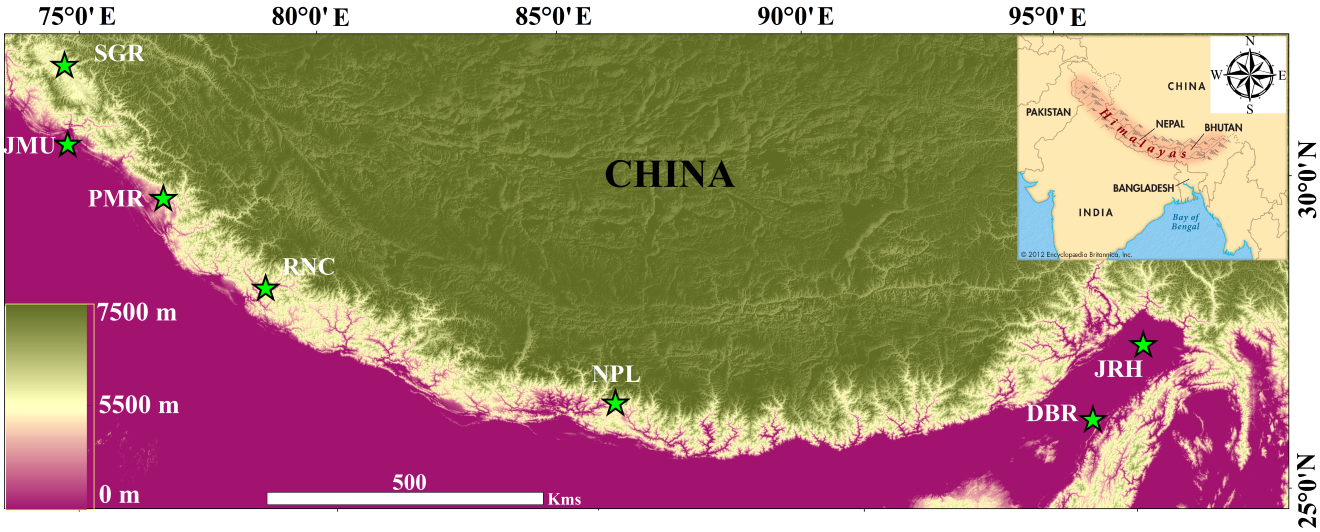

Figure 1. Locations of six sampling sites across the southern foothills of the Himalayas: SGR - Srinagar, JMU - Jammu, PMR - Palampur, RNC - Ranichauri, JRH - Jorhat and DBR - Dibrugarh. The position of Kathmandu station, Nepal (NPL), discussed in the text, is also marked in the figure.

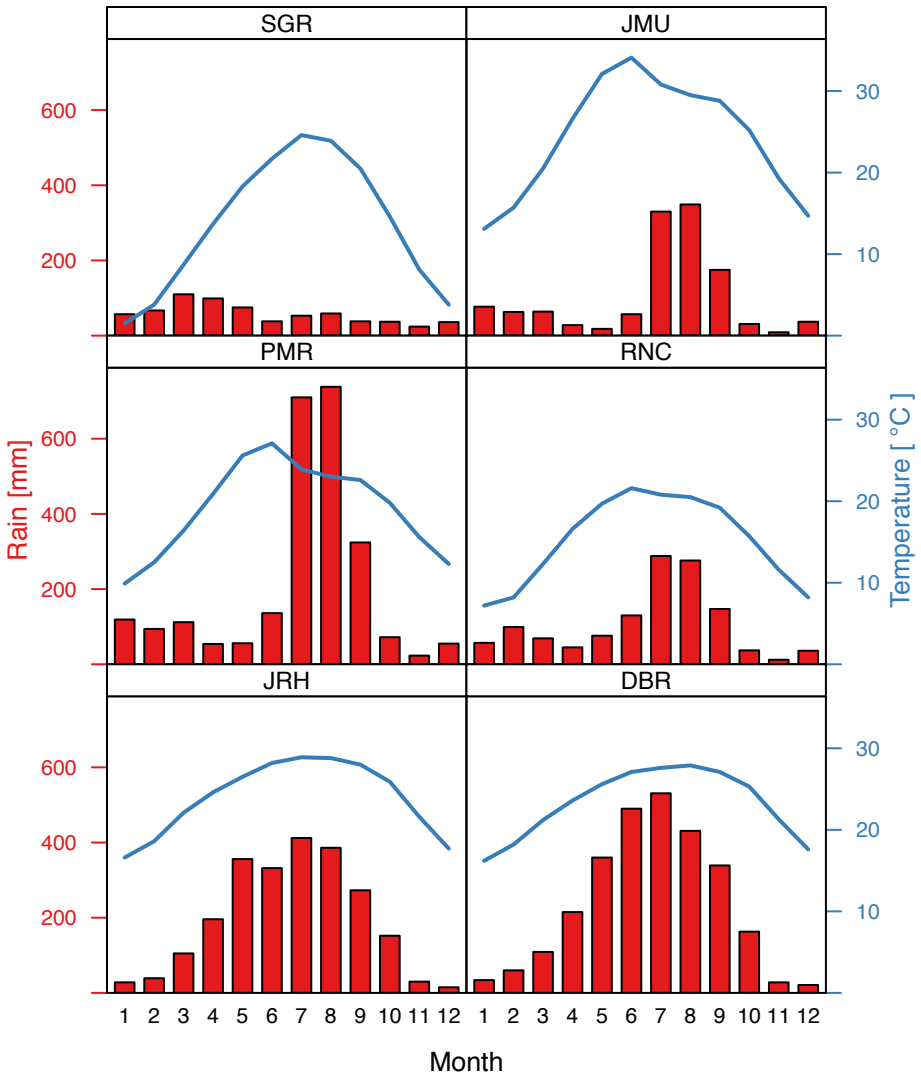

Figure 2. Long-term (1985-2014) monthly surface air temperature and precipitation data for six stations where daily sampling of rainfall for isotope analyses was conducted. SGR - Srinagar, JMU - Jammu, PMR - Palampur, RNC - Ranichauri, JRH - Jorhat, DBR - Dibrugarh. Source of data: Srinagar, Jammu, Palampur, Jorhat, Dibrugarh - pl.climate-data.org; Ranichauri - Upadhyay et al., 2015.

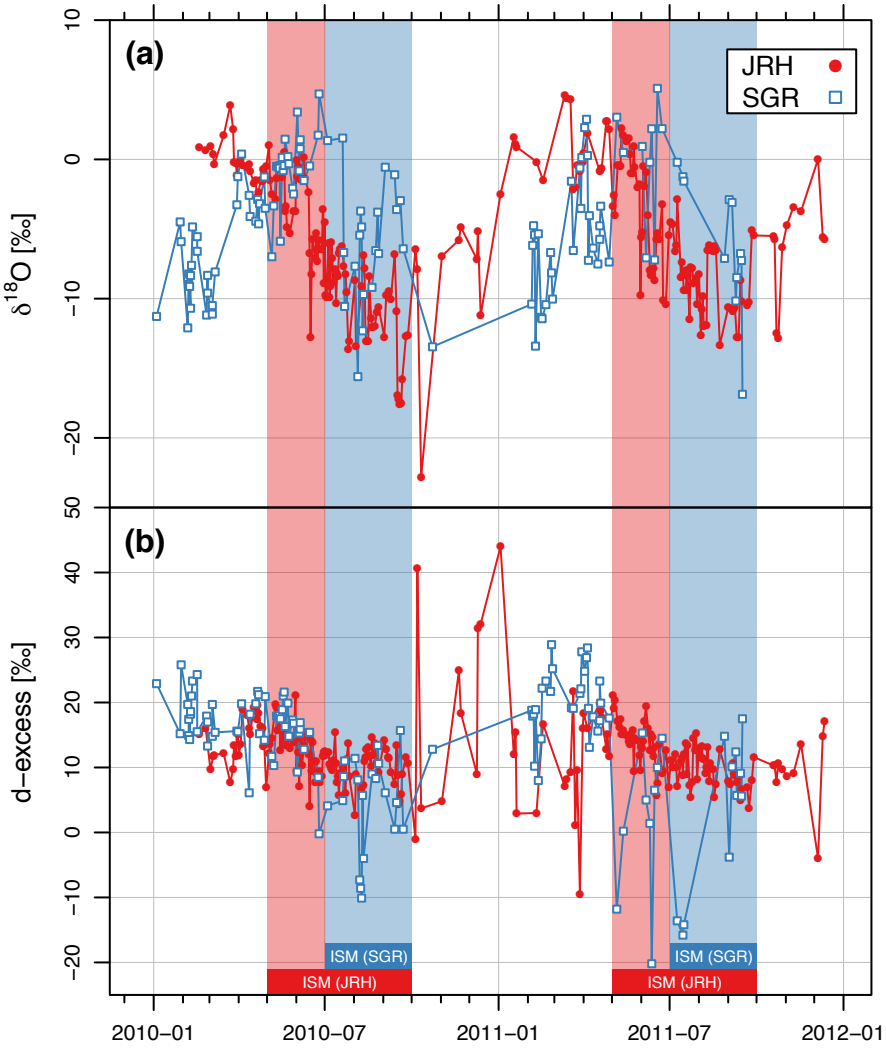

Figure 3. Seasonal variations of $\delta^{18}O$ (a) and d-excess (b) of daily rainfall collected at Jorhat (JRH) and Srinagar (SGR) stations. Indian Summer Monsoon (ISM) period at Srinagar (July-Sep) and Jorhat (May-Sep) is marked in blue and red shading, respectively.

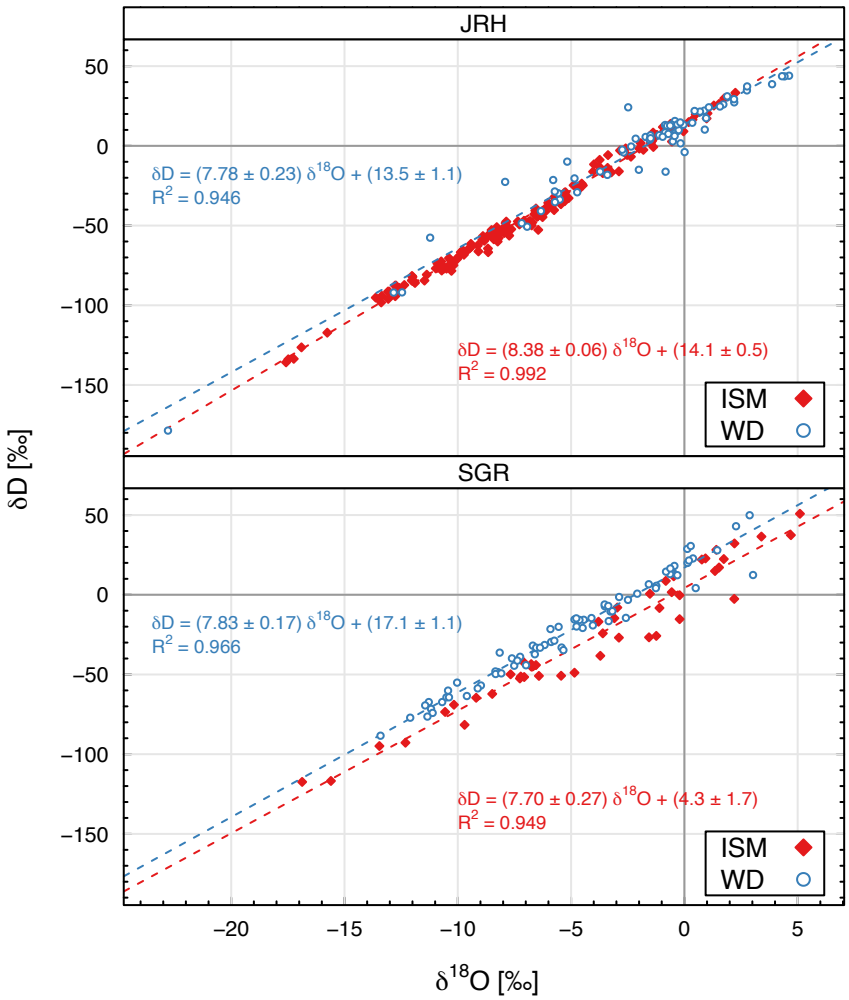

Figure 4. δ^2H - $\delta^{18}O$ relationship for daily isotope data available for Jorhat (JRH) and Srinagar (SGR) stations. Local Meteoric Water Lines were calculated separately for Indian Summer Monsoon (ISM) and Western Disturbances (WD) periods.

5

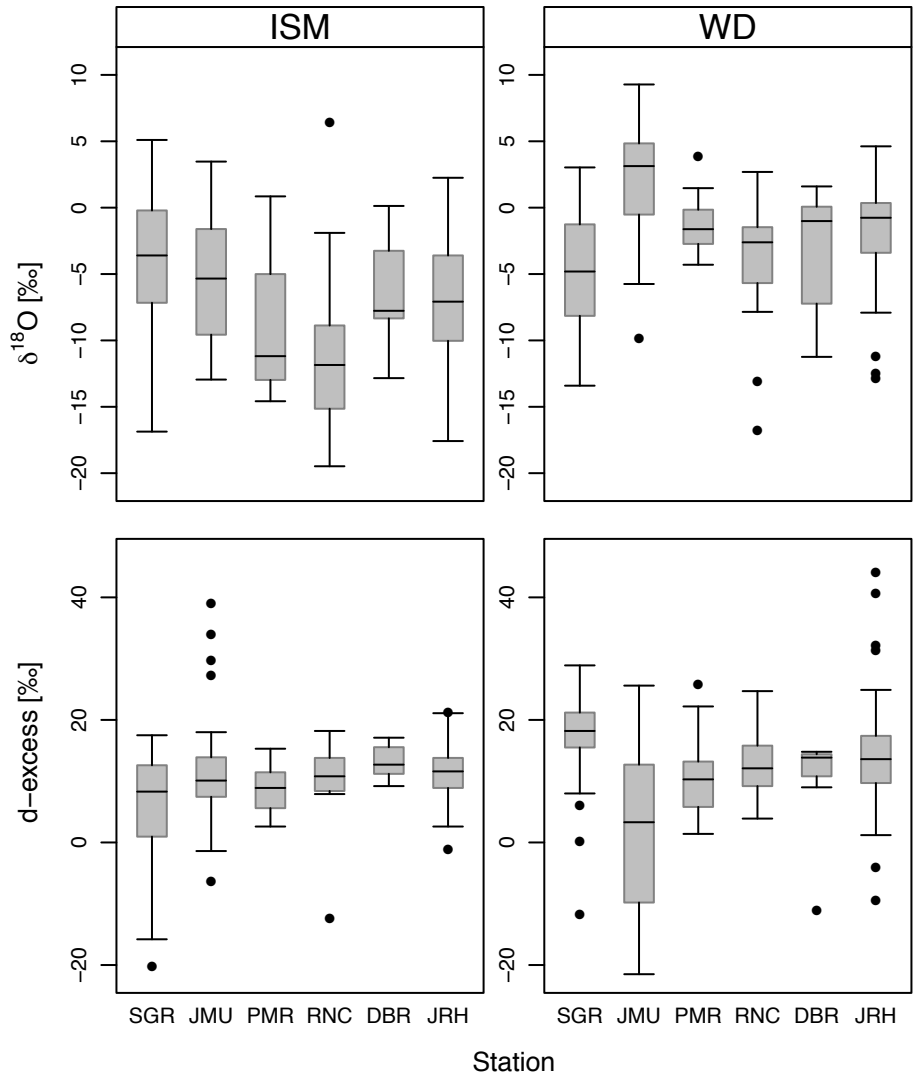

Figure 5. Box- and-whisker plots for $\delta^{18}O$ and d-excess values of daily rainfall at six stations (Srinagar - SGR; Jammu - JMU; Palampur - PMR; Ranichauri - RNC; Jorhat - JRH; Dibrugarh - DBR) collecting daily rainfall samples along southern foothills of the Himalayas (cf. Fig.1). The data are grouped into Indian Summer Monsoon (ISM) and Western Disturbances (WD) periods.

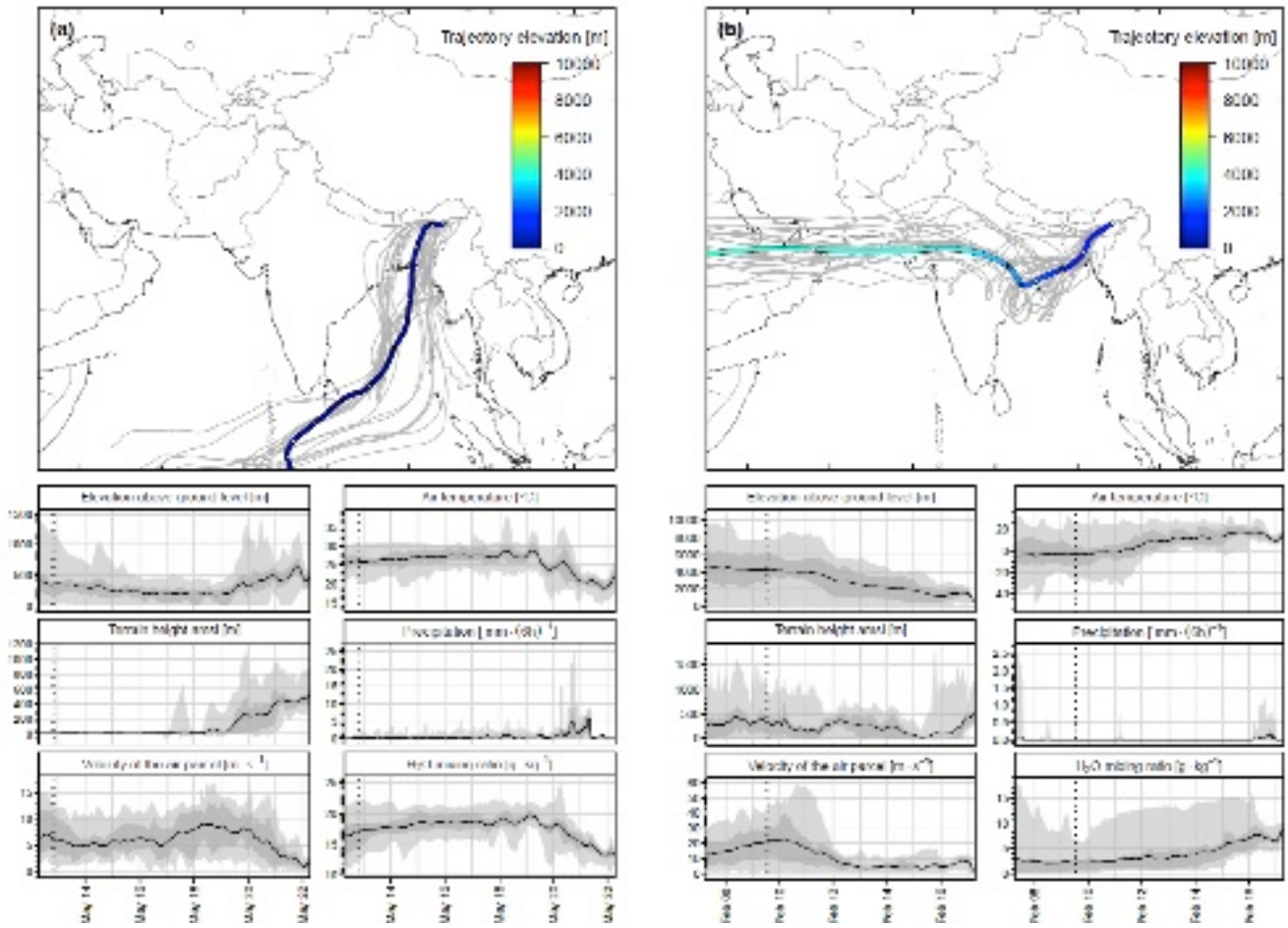

Figure 6. (a) upper diagram: 10-day backward trajectories arriving at Jorhat station on May 22, 2010, 12:00 hours and representing Indian Summer Monsoon (ISM) period. (b) upper diagram: 10-day backward trajectories arriving at Jorhat station on February 17, 2011, 12:00 hours and representing Western Disturbaces (WD) period. Twenty seven ensembles (grey lines in the background) and the mean trajectory (heavy line) are shown. Colours of the mean trajectory indicate elevation above the ground level in meters. Empty white dots on the mean trajectory indicate 24-hour intervals. Lower diagrams of (a) and (b) show the evolution of six selected parameters of air parcel along the trajectory. Evolution of the mean value of each parameter is marked in heavy black line and the associated uncertainty in grey. Dashed vertical lines mark part of the mean 10-day trajectory visible in the upper diagram. International boundaries are only indicative and as provided by the software.

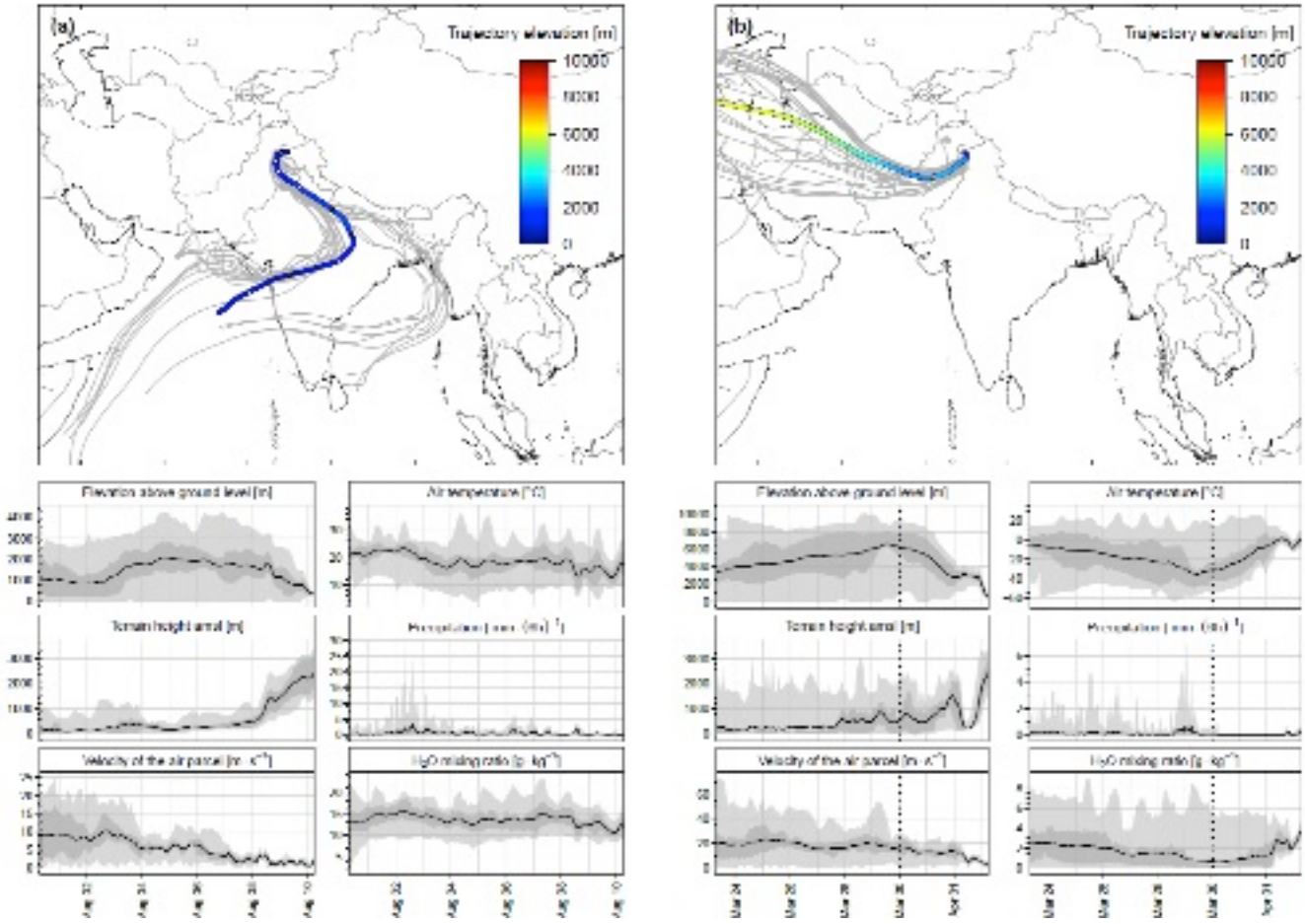

Figure 7. (a) upper diagram: 10-day backward trajectories arriving at Srinagar station on August 10, 2010, 12:00 hours and representing Indian Summer Monsoon (ISM) period. (b) Upper diagram: 10-day backward trajectories arriving at Srinagar station on April 2, 2011, 12:00 hours and representing Western Disturbaces (WD) period. Twenty seven ensembles (grey lines in the background) and the mean trajectory (heavy line) are shown. Colours of the mean trajectory indicate elevation above the local ground in meters. Empty white dots on the mean trajectory indicate 24-hour intervals. Lower diagrams of (a) and (b) show the evolution of six selected parameters of air parcel along the trajectory Evolution of the mean value of each parameter is marked by heavy black line and the associated uncertainty in grey. Dashed vertical lines mark part of the mean 10-day trajectory visible in the upper diagram. International boundaries are only indicative and as provided by the software.

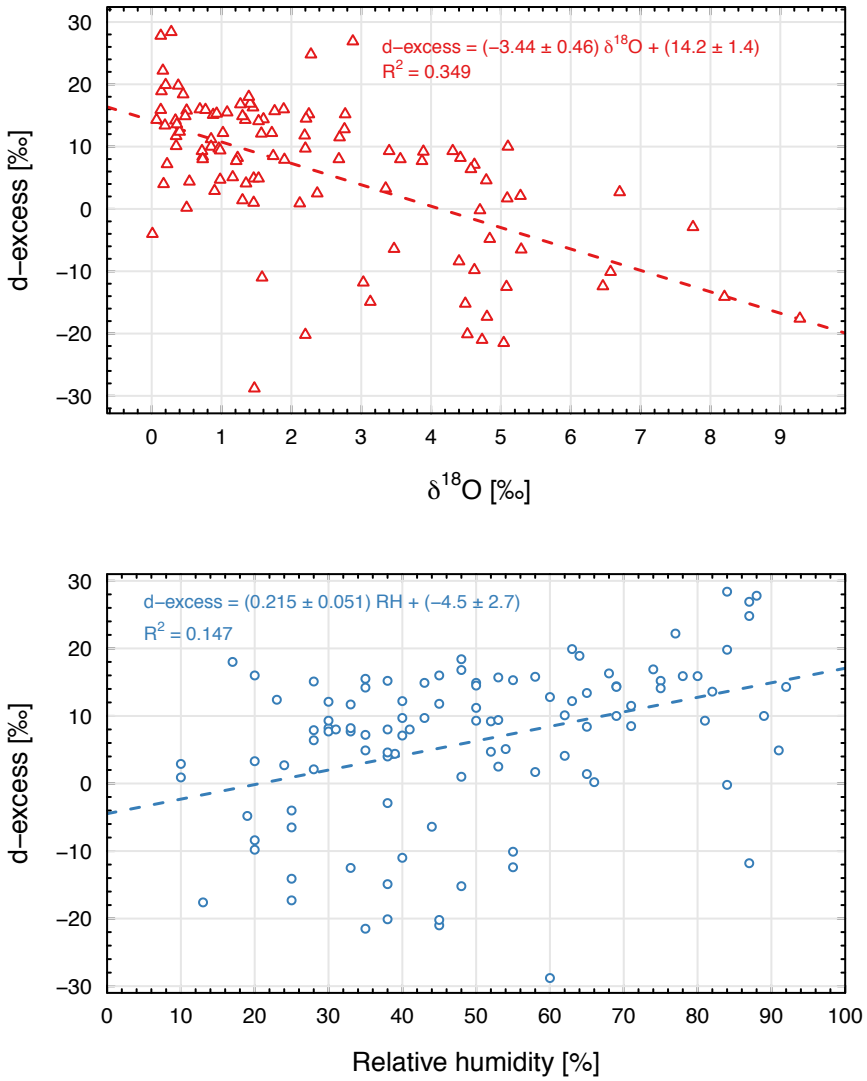

Figure 8. Upper diagram: relationship between deuterium excess and positive $\delta^{18}O$ values measured in daily precipitation samples collected by six stations distributed along southern foothills of the Himalayas (cf. Fig. 1). Lower diagram: relationship between deuterium excess and relative humidity of the local, near-ground atmosphere (daily means) calculated for precipitation events exhibiting positive $\delta^{18}O$ values.

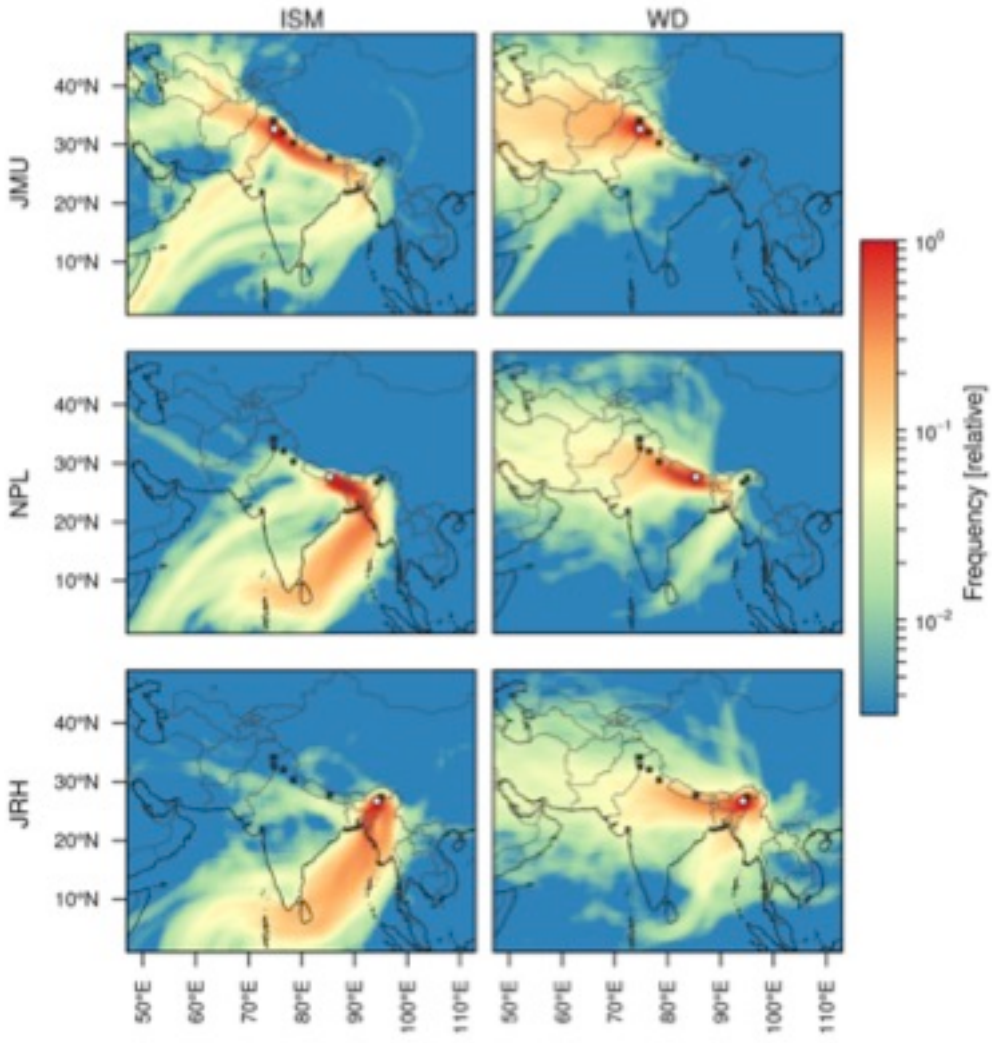

Figure 9. Footprint maps of air masses arriving at three stations: Jammu (JMU), Kathmandu (NPL) and Jorhat (JRH) representing western, central and eastern part of the studied east-west transect along southern foothills of the Himalayas, respectively (top, middle and bottom graphs). Separate maps were prepared for Indian Summer Monsoon (ISM) and Western Disturbances (WD) periods. Daily trajectories for the period 2009-2011 were reconstructed using Hysplit modelling framework (see text for details). International boundaries are only indicative and as provided by the software. Colour scale indicates the focally averaged number of trajectories passing through a grid cell.